CONSTRUCTION
E-ISSN: 2785-8731
VOLUME 5, ISSUE 1, 2025, 1 - 17
DOI: https://doi.org/10.15282/construction.v5i1.11407

RESEARCH ARTICLE

Rock Mass Classification and Geo-resistivity Properties of Granite from Pahang, Malaysia

A. F. Salmanfarsi and H. Awang*

Faculty of Civil Engineering Technology, Universiti Malaysia Pahang Al-Sultan Abdullah, 26300 Pahang, Malaysia

ABSTRACT - In tropical climate, exposed rocks are significantly weathered to form extensive weathering profile, which greatly affect the engineering integrity of the material. Geophysical method such as the electrical resistivity mapping have increasingly being used in the classification of the geoengineering properties of rock slope alongside conventional field and laboratory testing. In this study, comprehensive assessment of the weathered granite is carried out on selected exposed granite slopes in the Karak-Lanchang area, Pahang. Petrological analysis indicated quartz minerals as being the most stable mineral among the weathering grade. With increasing weathering grade, for physical properties of the granite of porosity and moisture content shows positive trend, whereas the specific gravity, slake durability index, and ultrasonic pulse velocity shows negative trend; for mechanical properties, the surface hardness rebound value, point load strength, and uniaxial compressive strength shows negative trend with increase of weathering grade. Mapping from the resistivity zones correlate with five zones of weathering grade, ranging from <200Ωm for Grade V and up to 3000Ωm for Grade I. The electrical resistivity value would also correspond to the different engineering properties of the weathered granite. Engineering properties results indicate the mechanical behaviour of high durability to very high durability and medium strength to very high strength of the rock material. Rock mass rating of the slopes fall under Class II ('good'). The results from electrical resistivity mapping, engineering tests, and rock mass classification indicate the slopes to be intact. From the results, a general geo-engineering properties of weathered granite is proposed.

ARTICLE HISTORY

Received	:	11th Oct. 2024
Revised	:	05th Dec. 2024
Accepted	:	23rd Apr. 2025
Published	:	02nd May 2025

KEYWORDS

Rock engineering properties
Granite
Rock mass rating
Electrical resistivity
Geo resistivity

1. INTRODUCTION

Malaysia, with its tropical climate that is hot and humid, have resulted in exposed rock slopes that rapidly weathers over time [1]. Weathering is the process which lead to rock is be broken down as a result of the movement of water through the hydrologic cycle [2], causing alteration of minerals and general disintegration of rock materials, which eventually leads to overall weakening of the rock mass. The early stages of weathering are usually indicated by changing in colour of the rock material, with the increase of weathering grade showing similar increase in the colour of the rock surface from slightly to highly discoloured [3]. The amount of discolouration of rock material usually indicates the degree of weathering, leading to difference of engineering properties, even if within the same rock mass [4]. As a result of the weathering process, the density and strength properties of the rock materials would greatly decrease; on the other hand, porosity, swelling coefficients, and friability of rock materials increases along with the increase in weathering grade [5]. Overall weathering of rocks leads to significance changes in engineering properties, leading increase in pore spaces and reduction in mass and strength. [6]. These events can result in rock mass erosion and rock material deposition on the slope, referred to as rock slope degradation. After excavation, cut slopes in rock masses will degrade owing to stress release and weathering. In the humid tropics such as Malaysia, intense chemical weathering would lead to high occurrence of landslides [7]. In Malaysia, a number of studies have studied the effect of weathering on granitic rocks, where it was reported that weathering leads to the breakdown of geomechanical properties of rocks. [8] compiled a list of significant landslides in Malaysia, noting several of the incident occur along rock slopes that consists of granitic rock.

The evaluation of rock slope stability is not straightforward due to various contributing factors to slope failures, such as the slope geometry, slope forming material strength, rock type, discontinuity, weathering rate, and groundwater level. One of the characteristics that leads to cut slope instability occurrences is cut slope degradation [9]. A rock mass is viewed as being anisotropic and discontinuous, where discontinuities that are produced from stresses due to tectonic activities or weathering effect would naturally occur in a rock mass [10]. These discontinuities would strongly influence the rock mass, affecting the strength, deformation, and permeability [11]. Thus, it can be said that discontinuity plays an important role in rock slope stability and affect its behaviour, and should be considered when assessing the properties of rock slopes. Conventionally assessment of rock slopes could be divided into kinematic analysis, limit equilibrium, numerical modelling, and empirical methods [12]. Case studies of previously published work on rock slope assessment in Malaysia indicate the kinematic analysis being the most widely used method, followed by stability rating and numerical analysis

***CORRESPONDING AUTHOR | H. Awang** | ✉ haryatiawang@umpsa.edu.my

[13]. The rock mass classification is one of the more prevalent metho in stability rating through empirical methods, due to its simplicity and ability to manage uncertainty when dealing with the condition of the slopes [14].

Given the importance of mapping the discontinuous elements of a rock slope to properly asses the stability, conventional field mapping, such as the commonly used scanline method, does have several disadvantages: they are time consuming, and in areas with high steep-faced rock slope, field mapping of the slopes is quite limited due to constraint of safe working space and unapproachability to higher part of slopes [15]. To address this limitation, geophysical mapping such as the electrical resistivity mapping are being incorporated into rock slope assessment. Several studies have used electrical resistivity in the mapping of granitic rock slopes, usually integrated with other geo-engineering studies [16-21].

A study was carried out to investigate the weathering condition of cut slopes at Lanchang-Karak area of Pahang, Malaysia. The purpose is to determine the engineering properties and rock mass properties of the weathered granite from a series of slope in Lanchang-Karak area. Field mapping which consists of discontinuity mapping, weathering grade identification, and electrical resistivity mapping were carried out. Laboratory tests which consist of petrographic analysis, specific gravity, water content, porosities, slake-durability test, ultrasonic velocities, surface hardness, point load test, and uniaxial compressive test were carried out for identifying the engineering properties of the granite slope. From the field and engineering tests, the stability of the rock slopes could be determined through the rock mass classification. The results were compared with other published engineering tests of weathered granite, and a general geo-engineering index of weathered granite is proposed.

2. METHODOLOGY

2.1 Study Area

The study area lies in the Central Belt area of Peninsular Malaysia (Figure 1), where the rock unit consist of a mix of Carboniferous to Permian aged sedimentary and metasedimentary rocks, Triassic interbedded sedimentary rocks and volcanic, Jurassic continental sedimentary deposits, and granitic bodies [22]. The rock units along the area includes the Tembeling Group, Semantan Formation, and Seri Jaya Beds, as well as volcanic and granite bodies [23,24]. The granites are predominantly of the I-type, formed during the geological period of Permian to Triassic and Upper Cretaceous [25]. Texture of the granite range from large grained, with equigranular primary texture, to porphyrytic biotite and hornblende granite [26]. The granite grain sizes range from medium sized to medium-coarse sized, with subhedral-granular texture, with most of the granite identified as being biotite granite [27]. The feldspar and biotite in the granite show alteration to clay minerals along with increase of weathering grade of the granite [6]. Geochemistry studies on the granite of Pahang are related to its role as parent rock for bauxite [28], and the concentration of rare earth elements in weathered granite [29]. The focus of this study will be on this granite, where the geo engineering and geo resistivity properties of the rock unit is studied.

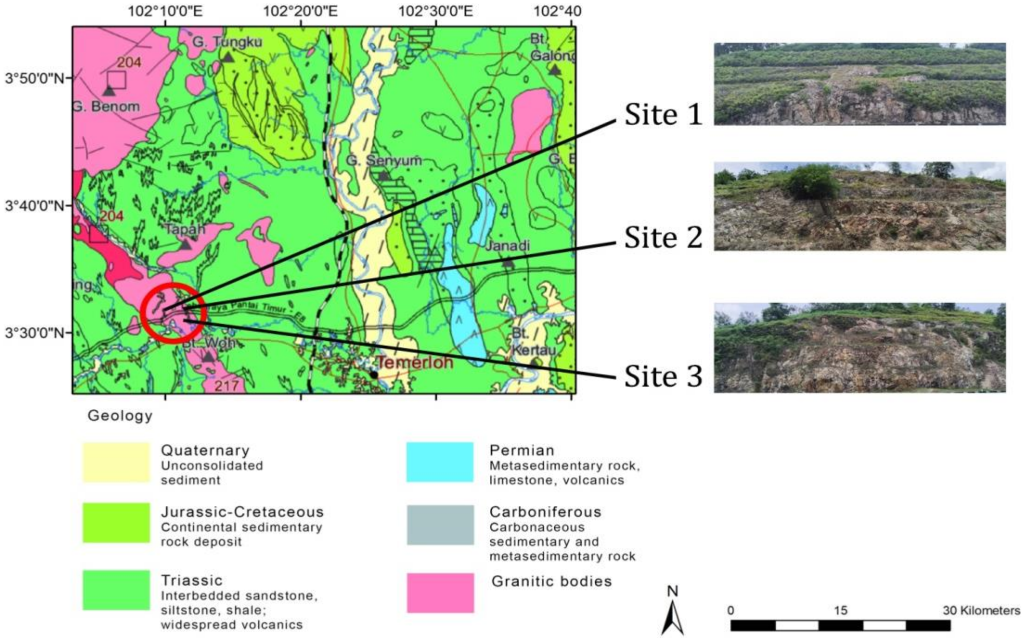

Figure 1. Geological rock unit along the Lanchang-Karak area. Geology from [22]

2.2 Field Data Collection

Field works were carried out on selected rock slope's in the study area. Rock samples were collected from the three (3) sites for laboratory tests, which are used for determining the engineering properties of the rock material and subsequently the assessment of the properties of the rock slopes. Sledge hammer was used to separate the blocks from the rock mass, according to the sizes suitable for laboratory engineering tests.

Rock slopes discontinuity mapping were carried out by implementing the scanline method by laying out measuring tape along the rock slopes, and keeping the tape as close as possible to the surface of the slope, as shown in Figure 2 (a). The dip and strike of joint and fractures, as well as other relevant parameters for analysis, were measured along the scanline. The discontinuity mapping method was conducted in accordance to the British Standards Institution (BSI) [30]. In addition, the weathering condition of the slopes were mapped. Investigation for the weathering condition of the rock slopes were carried out following the standard of BSI [31]. For each identified weathering grades, in-situ surface hardness tests were carried out using the Schmidt rebound hammer. Repeated reading of surface hardness were taken along the length of scanline, in order to quantify the weathering grade of the rock mass along the slopes, as shown in Figure 2 (b). A set of readings are taken for each section, with the application of the hammer to different part of the rock surface for each impact. Following the standards of International Society of Rock Mechanics (ISRM) [32]. measurement in group of 10s, with the 5 lowest reading discounted and averaging the highest 5 readings for discontinuity reading, were used to calculate the average reading for each measured section of the slopes.

(a) (b)

Figure 2. Field mapping of slopes. (a) Scanline mapping (b) Measurement of surface hardness of rock surface using Schmidt Rebound Hammer

2.3 Electrical Resistivity Mapping

Electrical resistivity mapping was carried out to identify the subsurface condition of the rock slopes. The electrical resistivity lines were set up using the ABEM Terrameter LS 2, connected to two multicore cables with stainless steel electrodes that are hammered into the ground in a generally straight line with constant spacing, connected to the ‘take out’ of the cables (Figure 3). The electrical resistivity mapping was carried out following the standards by ISRM [32] for land geophysics in rock engineering. The main unit ABEM Terrameter LS2 and 12 V battery, located at the centre of each surveying line. The resistivity lines was set out along roughly E-W alignment along rock slopes.

Testing configuration was based on the Schlumberger array, with the use of two (2) resistivity land cables and forty-one (41) electrodes. The Schlumberger array was used for the survey due to it providing dense near-surface coverage for resistivity data, with good vertical resolution and clear image of groundwater and sand-clay boundaries as horizontal structures [33].

Figure 3. Setting up of electrical resistivity mapping apparatus on the site

2.4 Laboratory Engineering Tests

Laboratory studies were carried out for identifying the mineralogy of the weathered granites, as well as determining the engineering properties of rock material from the identified weathering grades of the rock materials of the slopes (Figure 4). The tests that were conducted are petrographic analysis (for the purpose of rock identification and identification of mineralogical content), physical properties tests (covering the tests for specific gravity; water content; porosities; slake durability index, Id_2; and ultrasonic pulse velocity, UPV) and mechanical tests (covering the surface hardness using Schmidt Rebound Hammer, R; point load strength, PLS; and uniaxial compressive strength, UCS tests). The tests were carried out following the suggested methods for testing of rock materials by ISRM [32,34]

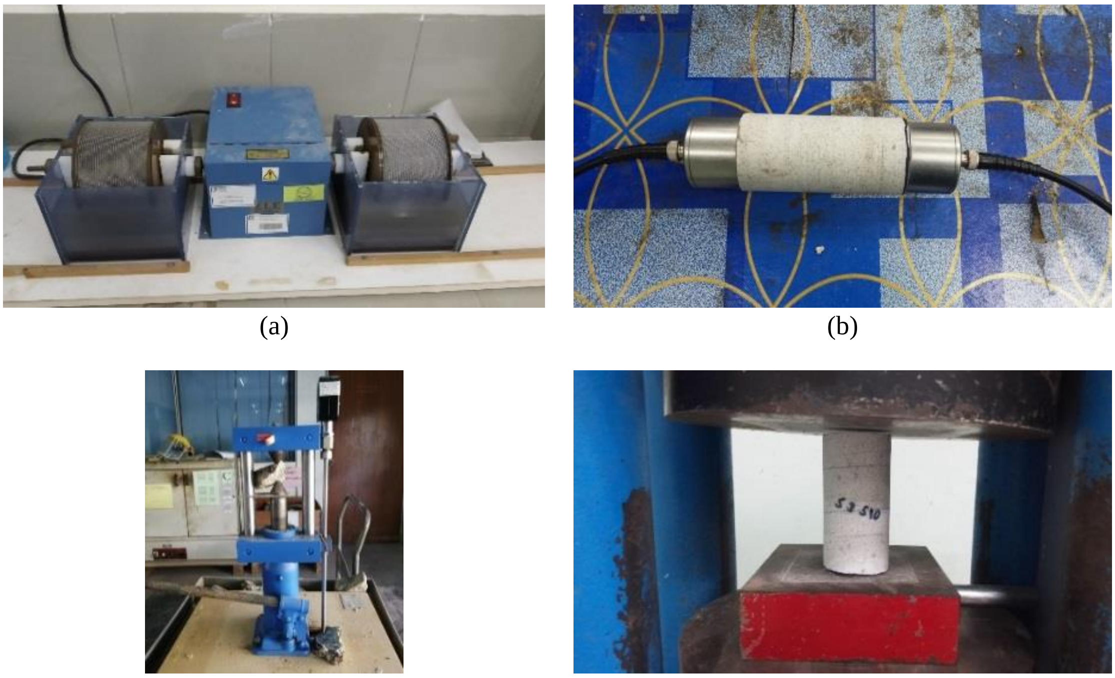

(a) (b)

(c) (d)

Figure 4. Laboratory testing apparatus for engineering tests. (a) Slake durability test (b) Ultrasonic pulse velocity test (c) Point load strength test (d) Uniaxial compressive strength test

2.5 Kinematic Analysis

Kinematic analysis is determined from the discontinuity mapping of the rock slopes. The concept of kinematic analysis is based on the Markland Test [35], where the probability of failures depends on the relationship between the slope dip angle and the internal friction angle of the rock mass [36]. The analysis was carried out using the software DIPS [37]. Using the software, the discontinuity data from the slopes could be plotted on stereonet plot, which makes it possible to identify an overall trend of the discontinuities on the slope. From the analysis, the potential for mode of failures (planar, wedge, and topping) for the different discontinuity sets are able to be determined.

2.6 Rock Mass Classification of Slope

From field mapping and laboratory tests, the rock mass classification of the slopes could be calculated. In this study, the Rock Mass Rating (RMR) is used, where several variations of the RMR is calculated where the different results are then compared. The original RMR, or RMR_{89} [38] is calculated using the sum of parameters of: strength of intact rock material (using either the input parameter of PLS or UCS) (R_δ), rock quality designation, or RQD (R_{RQD}), spacing between discontinuities (R_{SD}), condition of discontinuities (R_{CD}), and groundwater condition (R_{CG}). The equation is shown in Eq. 1:

$$RMR89 = R\delta + RRQD + RSD + RCD + RCG \tag{1}$$

The continuous function RMR, or the Modified-RMR (M-RMR) [39] uses the same parameter in RMR_{89} except that continuous function rating is used in place for each parameter, meaning that instead of a range of values for each parameter through discrete values ranking, the values are calculated using continuous functions to provide exact figures for each ranking of the parameters. This continuous function rating is applicable to both values of PLS reading (Eq. 2), or the UCS reading (Eq. 3) for the parameter of R_δ.

$$M - RMR = 0.2(RQD) + 15log(SD) + 1.670\,\delta + 2.9log\,(Groundwater\,flow) + 35.67 + RCD \tag{2}$$

$$M - RMR = 0.2(RQD) + 15log(SD) + 0.075\,\delta + 2.9log\,(Groundwater\,flow) + 34.00 + RCD \tag{3}$$

The 2014 RMR update (RMR_{14}) [40] follows discrete values ranking similar to RMR_{89} where several modifications were done: both parameter of R_{RQD} and R_{SD} were combined to form the density of discontinuities (R_{DD}) parameter; the rating for R_{CD} were modified to form the parameter R_{CD14}; and a new parameter for intact rock alterability rating (R_{IRA}) was added, using values from the slake durability tests. The equation of RMR_{14} is shown in Eq. 4.

$$RMR14 = R\delta + RDD + RCD14 + RIRA + RCG \tag{4}$$

3. EXPERIMENTAL RESULTS

3.1 Field Mapping of Rock Slopes

Surface hardness test on slope surface using Schmidt Rebound Hammer measures the rebound value, R, which are recorded alongside the weathering grade and the physical appearance of the rock surface. The slopes indicate weathering grade zone that range from Grade II to Grade V, with R values ranging between 10.8 to 67. To break down each weathering grade and the observed R values, section of slopes with grade II granite shows R values between 41.2 and 67; granite of Grade III show R value between 27.6 and 41; granite of Grade IV show R value of 10.8 to 21.5; Grade V granite returns no R value, and were highly weathered to brownish red soil material covered with vegetation. A summary of the weathering grade mapping is presented in Table 1. From the tabulated data, a general trend is that higher weathering grade of slope surface correspond to more deterioration of rock material and lower R values.

Table 1. Summary of weathering grade and Schmidt rebound hammer values from Site 1 – Site 3

Study area	Weathering grade, WG	Percentage	Mean	Min	Max	Standard deviation
Site 1	II	42.11	50.6	41.2	64.6	7.60
	III	36.84	33.3	27.6	40.2	5.40
	IV	5.26	10.8	10.8	10.8	-
	V	15.79	-	-	-	-
Site 2	II	33.33	56.8	45.8	67.0	6.19
	III	44.44	36.2	27.6	41.0	4.60
	IV	5.56	19.5	17.4	21.5	2.90
	V	2.78	-	-	-	-
Site 3	II	64.29	55.3	45.8	64.0	5.12
	III	28.57	40.3	39.6	41.0	0.57
	IV	7.14	17.6	17.6	17.6	-
	V	64.29	55.3	45.8	64.0	5.12

From discontinuity scanline mapping, several sets of discontinuities were identified, as summarized in Table 2. Discontinuity density, and Rock Quality Designation, RQD, which are necessary parameter for RMR, is also calculated and presented in the table.

Table 2. Summary of discontinuity data sets from Site 1 – Site 3

Study area	Discontinuity set	Dip (°)	Dip direction (°)	Discontinuity density (%)	Discontinuity density (m^{-1})	Rock Quality Designation, RQD (%)
Site 1	1	31	051	22.08	1.44	RQD = 115- 3.3 (7.74)
	2	78	064	13.75	1.13	= 87.10
	3	78	092	11.25	1.56	
	4	79	182	12.50	0.71	
	5	81	222	13.33	1.50	
	6	72	263	20.00	1.40	
Site 2	1	75	033	34.87	1.81	RQD = 115- 3.3 (21.46)
		34	054	14.47	2.37	= 44.20
	3	89	074	5.263	1.62	
	4	78	178	4.61	14.29	
	5	55	275	4.61	1.37	
Site 3	1	73	045	41.03	2.34	RQD = 115- 3.3 (7.28)
	2	56	135	13.10	2.31	= 91.01
	3	71	253	23.10	2.63	

3.2 Petrographic Analysis

Petrographic analysis of weathered rock samples was carried out to identify the changes in mineral composition and textures across the weathering grades. The result of petrographic analysis is shown in Figure 5 and Table 3:

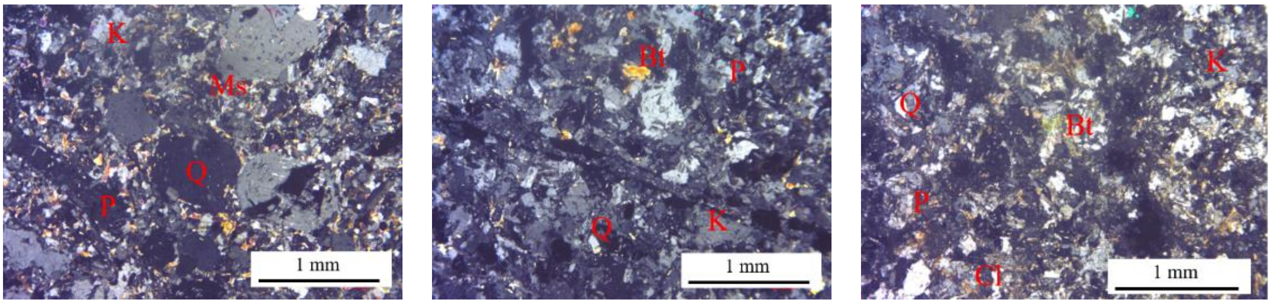

(a) (b) (c)

Figure 5. Photomicrograph of granite samples from study area: (a) Weathering Grade II (WG II) (b) Weathering Grade III (WG III) (c) Weathering Grade IV (WG IV)

Table 3. Summary of main mineral content of weathered granite for studied area

Weathering grade, WG	Quartz (Q)	K-feldspar (K)	Plagioclase (P)	Mica: Biotite (Bt)/ Muscovite (Ms)/ Chlorite (Cl)
II	52.85-73.64	9.79-26.66	6.08-12.85	1.25-9.69
III	60.00-66.98	20.95-22.05	6.66	5.39
IV	54.00-57.23	22.66-32.15	1.60-5.00	3.53

From field observation and petrographic analysis, the rock is identified as medium-coarse grained granite, with quartz and feldspar being the primary minerals that make up the rock. Biotite occurs as accessories minerals, as well as smaller occurrence of hornblende. Quartz mineral range in size from 2 to 4 mm. In Grade II granite, the quartz shows no sign of weathering, whereas feldspar mineral show alteration around its edges in the formation of sericite mineral (sericization). With increasing grade of weathering, quartz grains commonly exhibit more fractures, and starts to be crystallized in polycrystalline form (i.e. smaller group of grains). Feldspar shows greater alteration into sericite, and biotite minerals are altered into greenish chlorite. In Grade IV, majority of feldspar and biotite is altered into fine clayey minerals, which forms the groundmass of the rock. Iron oxide minerals becomes quite prominent in the groundmass, filling in the spaces as opaque spots. Quartz remains unchanged in this weathering grade compared to other minerals. For Grade V, the granite samples are too fragile to be prepared for thin sections.

3.3 Engineering Properties

Engineering properties tests carried out for the rock materials involves the measurement of specific gravity, moisture content, porosity, slake durability index, and pulse velocity. The relationship between the physical properties and the weathering grade of the granite, as well as the relationship between the slake durability index and pulse velocity against weathering grade of the granite, is shown in Figure 6 to Figure 8.

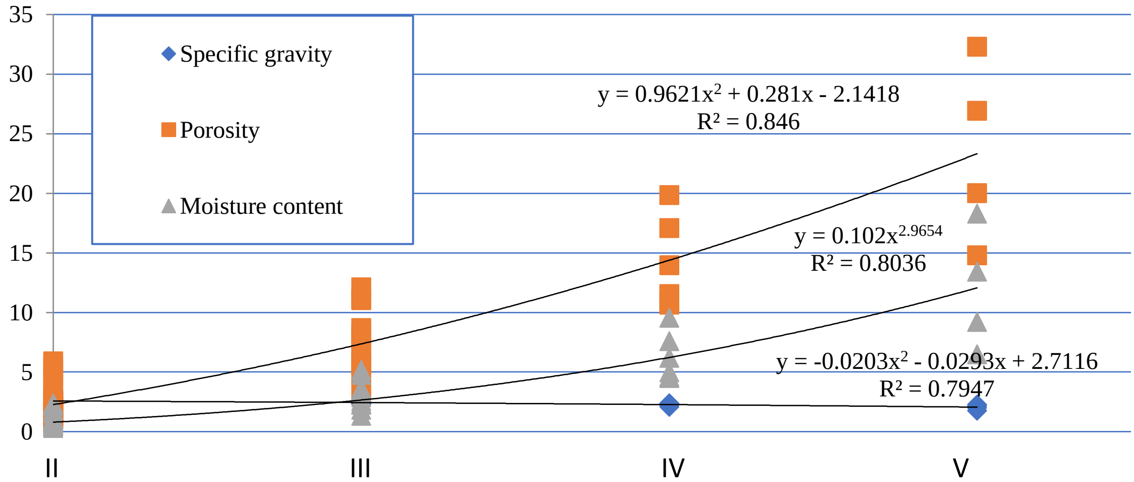

Figure 6. Relationship between the physical properties and the weathering grade of granite samples from Lanchang-Karak. From top to bottom: porosity VS weathering grade, moisture content VS weathering grade, and specific gravity VS weathering grade

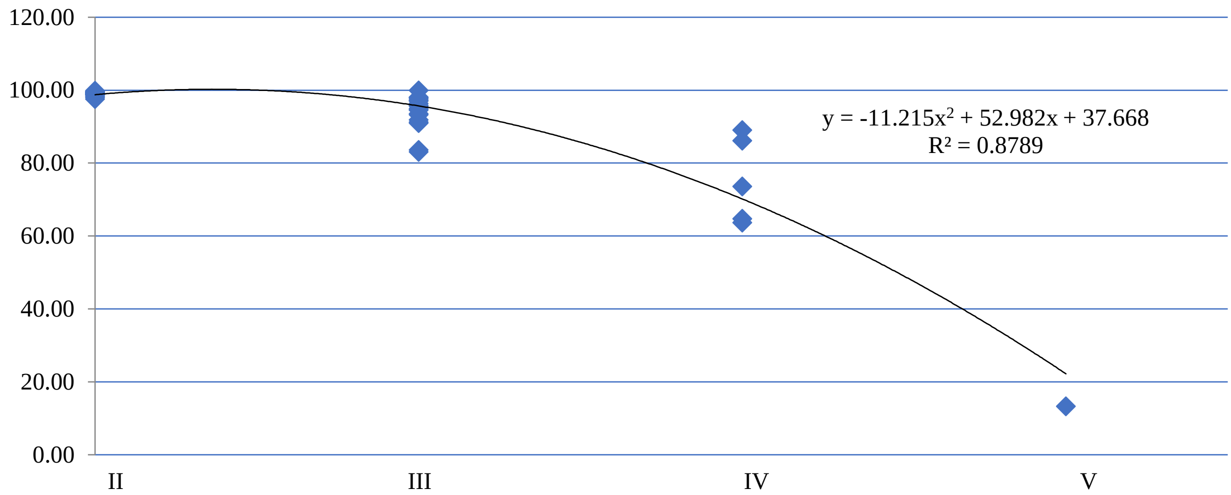

Figure 7. Relationship between slake durability index and the weathering grade of granite samples from Lanchang-Karak

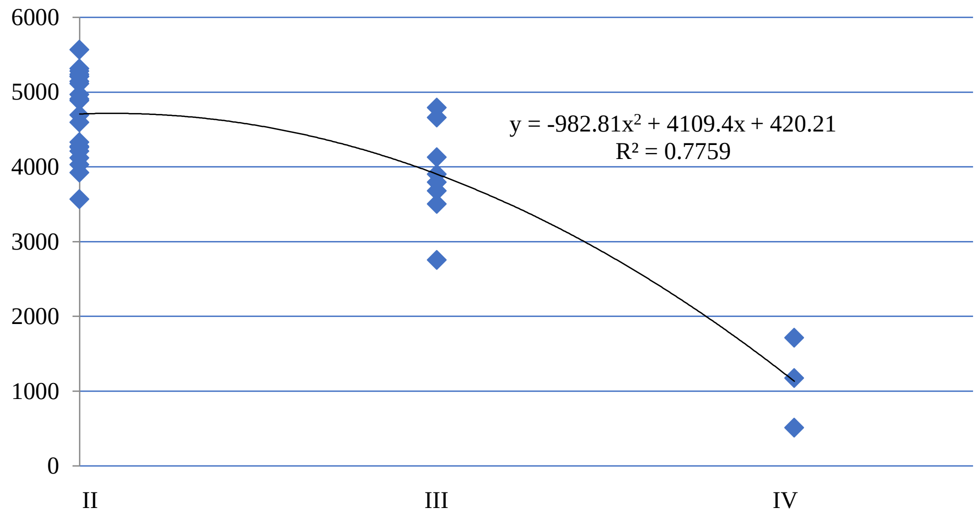

Figure 8. Relationship between ultrasonic pulse velocity and the weathering grade of granite samples from Lanchang-Karak

A summary of the mean value of the measured parameters is shown in Table 4, and a summary of the statistical analysis of the data set is shown in Table 5. The mean specific gravity values for weathered granite are 2.57 g/cm^3, 2.44 g/cm^3, 2.27 g/cm3 and 2.06 g/cm^3 for Grade II, III, IV and V respectively. The mean porosity values are 2.24%, 7.53%, 14.00%, and 23.51% for weathering Grade II, III, IV, and V respectively. The mean moisture content values are 0.88%, 3.12%,6.24%, and 23.51% for Grade II, III, IV, and V respectively. The mean slake durability for weathered granite are 99.07%, 94.58%, 75.48% and 13.34% for Grade II, III, IV and V respectively. The mean pulse velocity are 5726.21 m/s, 4131.40 m/s, and 1196.01 m/s for Grade II, III, and IV respectively. The general trend indicates that with an increasing grade of weathering in granite, there is statistically significant increase in the porosity and moisture content of the granite. On the other hand, with increase of weathering grade of granite, there is statistically significant decrease in the specific gravity, slake durability index, and pulse velocity of the granite. Interpretation of the observed behaviour is that the increase of weathering grade causes degradation of the mineral grains in the material, leading to formation of pores which would subsequently increase the amount of water content and causes significant loss of rock materials, which in turn is reflected in lower mass and weaker strength.

Collected rock samples from different weathering grades were subjected to different mechanical/strength tests. The carried out tests are the and slake-durability test, laboratory surface hardness test (Schmidt rebound hammer, R), point strength (PLS) test, and uniaxial compressive strength (UCS) test. The relationship between the mechanical properties and the weathering grade of the granite is shown in Figure 9.

Table 4. Summary of physical properties of Lanchang-Karak granite

Properties	Weathering grade, WG	Mean	Min	Max	Standard deviation	Skewness
Specific gravity, SG (g/cm^3)	II	2.57	2.47	2.63	0.04	Negative
	III	2.44	2.30	2.56	0.08	Negative
	IV	2.27	2.08	2.37	0.11	Negative
	V	2.06	1.77	2.29	0.22	Negative
Porosity, n (%)	II	2.24	0.80	5.90	1.20	Positive
	III	7.53	1.65	12.10	2.67	Positive
	IV	14.00	8.06	20.75	3.77	Positive
	V	23.51	14.79	32.31	7.69	Positive
Moisture content, MC (%)	II	0.88	0.31	2.39	0.49	Positive
	III	3.12	1.33	5.17	1.20	Positive
	IV	6.24	4.49	9.55	2.00	Positive
	V	11.85	6.49	18.28	5.15	Positive
Slake durability index, Id_2 (%)	II	99.07	97.62	99.85	0.66	Negative
	III	94.58	91.29	99.98	2.00	Negative
	IV	75.48	63.74	89.10	8.08	Negative
	V	13.34	13.34	13.34	-	-
Pulse velocity, Vp (m/s)	II	4726.21	4030.30	5316.58	471.51	Negative
	III	4131.40	3505.25	4794.37	505.36	Negative
	IV	1196.01	511.35	1713.96	507.71	Negative

Table 5. Summary of correlation between physical properties and weathering grade of Lanchang-Karak granite

Physical properties	Degree of freedom, df	t-test value	P-value	Correlation, r
SG	53	13.91	0	-0.89
n	53	16.20	0	0.91
MC	53	13.36	0	0.88
Id_2	55	8.57	0	-0.76
Vp	30	7.92	0	-0.82

A summary of the mean value of the parameters for the different weathering grade is shown in Table 6 and a summary of the statistical analysis of the data set is shown in Table 7.

Table 6. Summary of mechanical properties of Lanchang-Karak granite

Properties	Weathering grade, WG	Mean	Min	Max	Standard deviation	Skewness
Rebound Hammer value, R	II	53.20	42.00	64.00	7.40	Positive
	III	40.00	34.60	44.80	3.70	Negative
	IV	17.00	14.00	19.40	2.80	Positive
Point Load Strength, PLS (MPa)	II	5.48	2.95	11.36	2.09	Positive
	III	1.00	0.20	3.55	0.71	Positive
	IV	0.18	0.06	0.36	0.06	Positive
	V	0.06	0.06	0.06	-	-
Uniaxial Compressive Strength, UCS (MPa)	II	87.57	68.31	100.85	11.65	Negative
	III	73.59	59.19	88.84	11.62	Positive
	IV	11.78	5.56	17.99	8.79	Positive

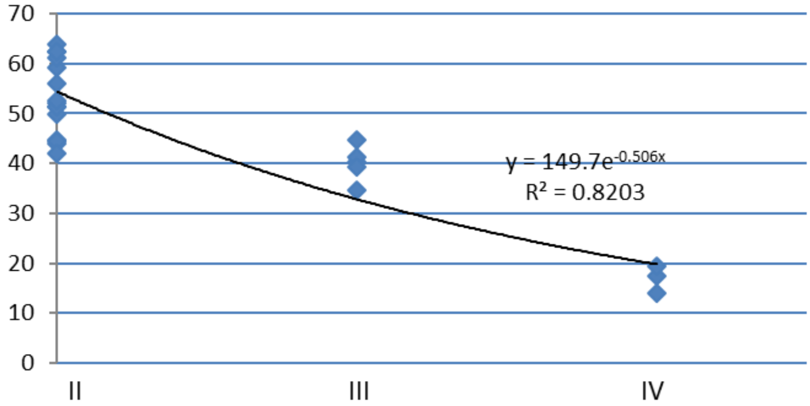

(a)

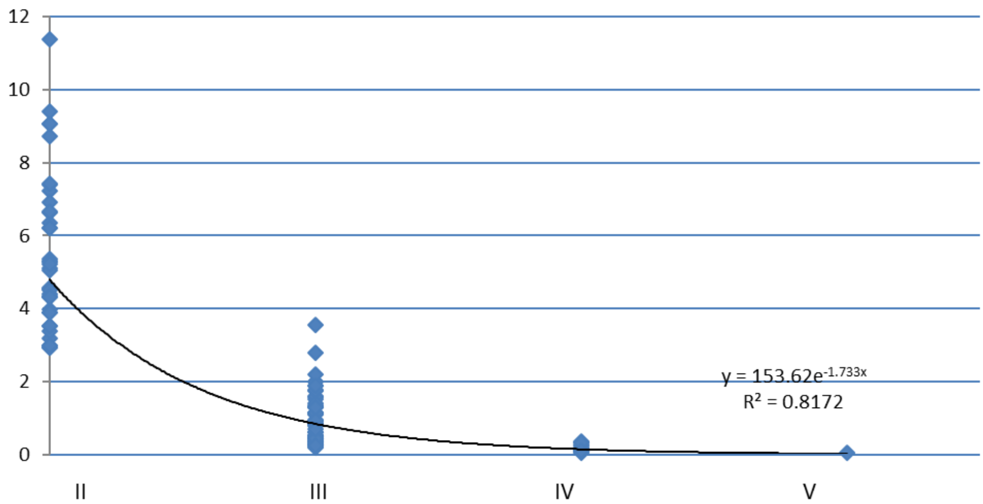

(b)

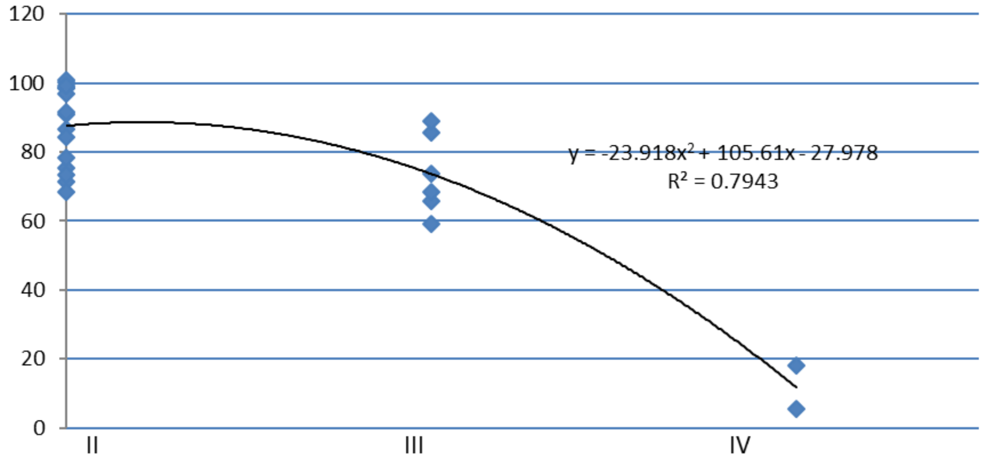

(c)

Figure 9. Relationship between the engineering properties and the weathering grade of granite samples from Lanchang-Karak (a) R VS weathering grade, (b) PLS VS weathering grade, and (c) UCS VS weathering grade

Table 7. Summary of correlation between strength properties and weathering grade of Lanchang-Karak granite

Strength properties	Degree of freedom, df	t-test value	P-value	Correlation, r
R	21	8.76	0	-0.89
PLS	73	8.94	0	-0.72
UCS	21	6.25	0	-0.81

The Schmidt rebound hammer values are 42.0-64.0, 34.6-44.8, and 14.0-19.4 for weathering grade II, III, IV, with no values returned for grade V. The mean point load strength values are 5.48 Mpa, 1.00 Mpa, 0.18 Mpa, and 0.06 Mpa for grade II, III, IV, and V. The mean uniaxial compressive strength values are 87.57 Mpa, 73.59 Mpa, and 11.78 Mpa for grade II, III, and IV. The general trend indicates that with an increase of weathering grade of granite, there is statistically significant decrease in the strength properties of the granite. Interpretation of the observed behaviour is that strength of the rock material is affected by the overall density of the material: the increase of weathering grade causes degradation of the mineral grains in the material, leading to increase of porosity and moisture content which would overall severely degrade the strength of the material.

3.4 Electrical Resistivity Profile of Weathered Granite

Electrical resistivity survey was conducted along a 100 m line for Site 1 and 200 m line for Site 2 and Site 3. Due to the limitation of the length of slope surface that is accessible for the surveying, the electrical resistivity survey was carried out with an electrode spacing of 2.5 meter for Site 1 and 5 meters for Site 2 and Site 3 respectively. With this configuration, the maximum depth of the image reaches up to 20 for Site 1 and 40 m for Site 2 and Site 3. The profile of the electrical resistivity mapping and interpretation of the resistivity profile is as shown in Figure 10 to Figure 12:

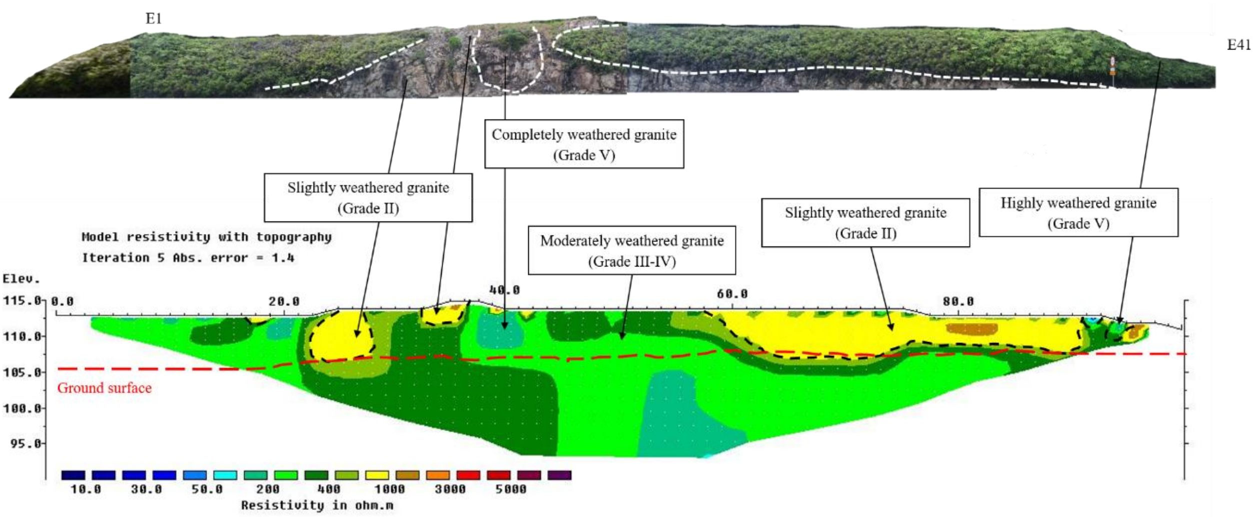

Figure 10. Electrical resistivity profile and interpretation for Site 1

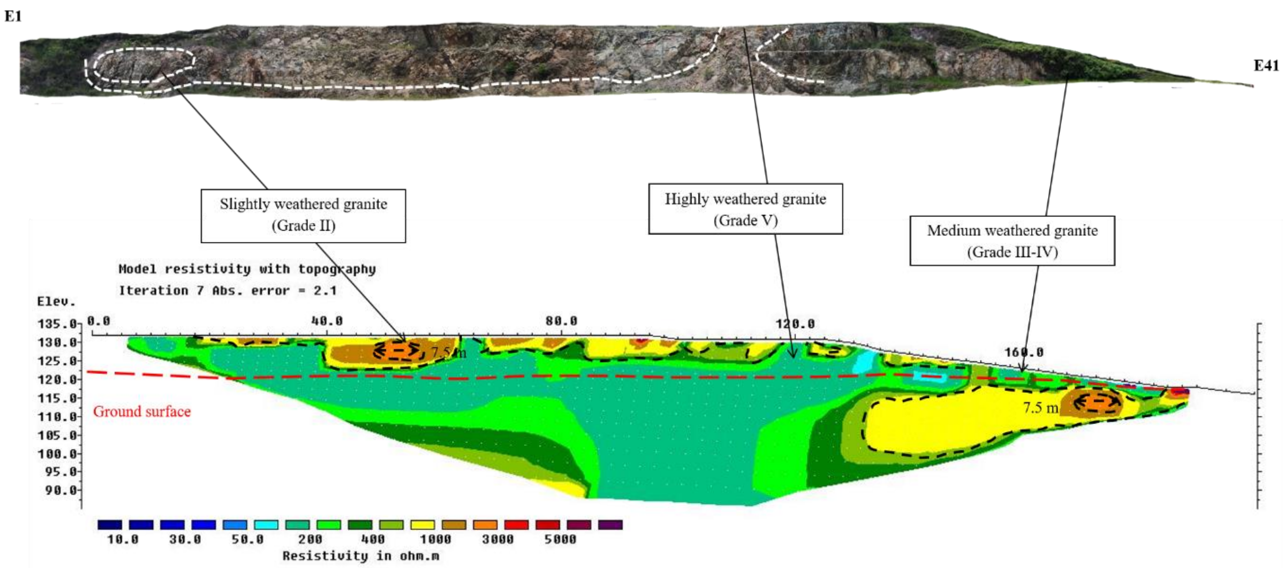

Figure 11. Electrical resistivity profile and interpretation for Site 2

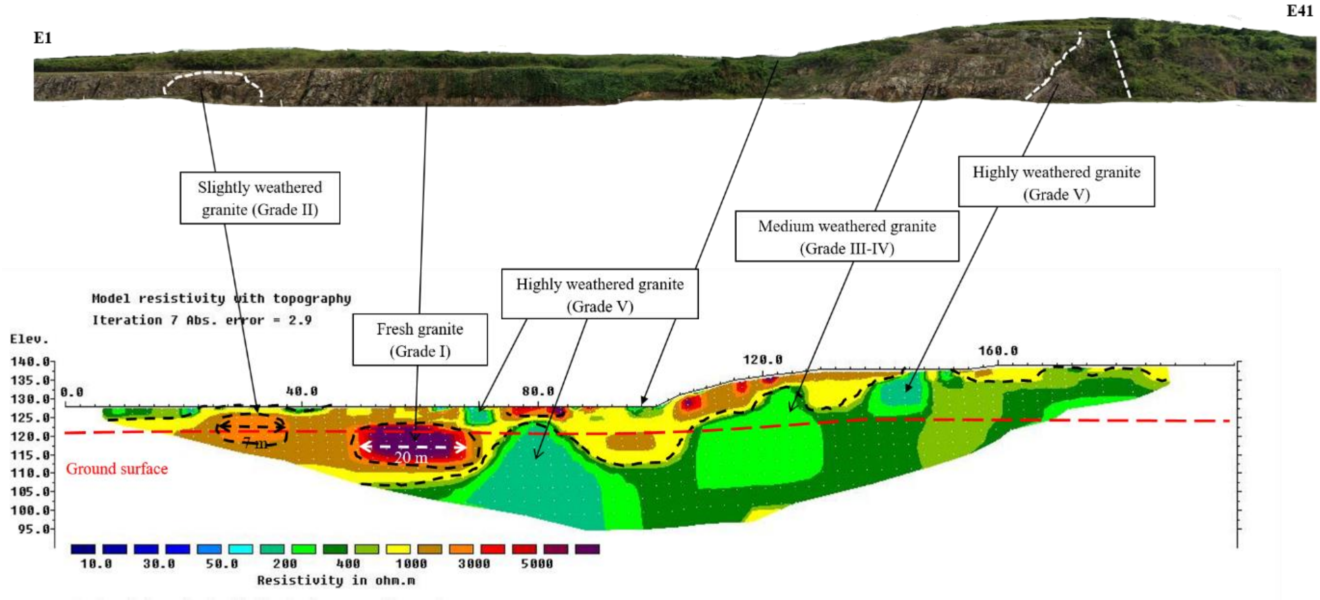

Figure 12. Electrical resistivity profile and interpretation for Site 3

For Site 1, a zone of resistivity value greater than 1000 Ωm – represented by yellow and brown in the electrical resistivity profile – is found around the right side and centre of the slope, corresponding to blocky granite exposure with discontinuity sets, and are interpreted to be slightly weathered granite zone. The second zone, with resistivity value in the range of 300 – 1000 Ωm – represented light-green to greenish yellow in the electrical resistivity profile – is found in the left and centre section of the slope, and are interpreted to be medium-weathered granite zone as it corresponds to the weathered granite surfaces with discontinuity sets. The third zone, with resistivity value less than 300 Ωm – represented by bluish green in the electrical resistivity profile – is found at the centre of the slope around 40 m length of the survey line is interpreted to be the highly weathered granite zone, as it corresponds to section of granite weathered to form dark reddish surface.

For Site 2, a zone of resistivity value greater than 1000 Ωm – represented by yellow and brown in the electrical resistivity profile – is found around the 47-55 m length of the survey line, corresponding to blocky granite exposure with discontinuity sets, and are interpreted to be slightly weathered granite zone. The second zone, with resistivity value in the range of 200 – 1000 Ωm – represented light dark green to greenish yellow in the electrical resistivity profile – is found in the lower centre part and right part of the slope, and are interpreted to be medium-weathered granite zone as it corresponds to the weathered granite surfaces with closely spaced discontinuity sets. The third zone, with resistivity value less than 200 Ωm – represented by bluish green in the electrical resistivity profile – is found at the centre of the slope around the 120 m length of the survey line is interpreted to be the highly weathered granite zone, corresponding to zone of intact granite material covered with weak and loose rock materials.

For Site 3, a zone of resistivity value greater than 1000 Ωm – represented by yellow and brown in the electrical resistivity profile – is found around the majority of the upper section of the slope, corresponding to blocky granite exposure with discontinuity sets, and are interpreted to be slightly weathered granite zone. The second zone, with resistivity value in the range of 200 – 1000 Ωm – represented light-dark green to greenish yellow in the electrical resistivity profile – is found in the left section and lower part of the right section of the slope, and are interpreted to be medium-weathered granite zone as it corresponds to the weathered granite surfaces with discontinuity sets. The third zone, with resistivity value less than 200 Ωm – represented by bluish green in the electrical resistivity profile – is found at the upper part of the left section and center section of the slope, is interpreted to be the highly weathered granite zone, as it corresponds to zones where intact granite blocks are surrounded by loose and weak materials.

Based on the comparison between the mapped slope surface and the electrical resistivity profile, the difference in the values of electrical resistivity could be attributed to the condition of the rock material of the slopes, caused due to the different state of weathering. Results of laboratory testing from the previous section show that there is high degree of correlation between the weathering grade of granite and the engineering properties of the material, with an observed decrease in strength and increase of moisture content with the increase of weathering grade. Although out of the scope of this paper, several laboratory studies between measured electrical resistivity of rock material and engineering properties have noted on the correlation between electrical resistivity with the engineering properties, with increase of electrical resistivity related to increase of strength and decrease in physical properties of rock materials [41-43]. Therefore, when dealing with mapping of rock body where changes of rock type can be ruled out for the observed different zones of electrical resistivity, the different zones can be attributed to different grade of weathering of the rock, each showing distinct engineering properties. From the subsurface interpretation and surface observation of the rock slope, a range of electrical resistivity values and interpreted weathering grades proposed, as in Table 8.

Table 8. Proposed resistivity range for weathering grade of granite for Site 1 – Site 3

Location	Weathering grade, WG	Material description	Resistivity (Ωm)
Site 1	II	Slightly weathered	1000-3000
	III	Moderately weathered	400-1000
	IV	Highly weathered	300-400
	V	Completely weathered	<300
Site 2	II	Slightly weathered	1000-3000
	III	Moderately weathered	400-1000
	IV	Highly weathered	200-400
	V	Completely weathered	<200
Site 3	I	Fresh rock	>3000
	II	Slightly weathered	1000-3000
	III	Moderately weathered	400-1000
	IV	Highly weathered	200-400
	V	Completely weathered	<300

3.5 Kinematic Analysis

Kinematic analysis of these discontinuities was carried out, in order to identify the potential of kinematic failures for the slopes. The summary of the analysis is shown in Table 9. From the result, it can be summarized that there is very low potential of planar failures to occur due to the discontinuity sets in the rock mass; meanwhile there are significance potential of wedge failures, and low potential for toppling to occur due to the orientation of the discontinuity sets in the rock mass.

Table 9. Summary of kinematic analysis of rock slopes from Site 1 – Site 3

Slope	Planar (%)	Wedge (%)	Toppling (Flexural) (%)	Toppling (Direct) (%)
Site 1	0.42	15.53	1.67	15.64
Site 2	0.00	11.66	3.29	24.02
Site 3	0.00	19.94	6.90	14.16

3.6 Rock Mass Classification

Results from the field mapping and laboratory tests are used for the evaluation of RMR. The evaluation of the RMR Table 10.

Table 10. Evaluation of Rock Mass Rating for Site 1 – Site 3

Parameters	Description or values	Rating: RMR_{89}/ M-RMR/RMR_{14}	RMR_{89}	M-RMR	RMR_{14}
Site 1					
Point load test ($I_{s(50)}$) (Mpa)	1.56 - 7.40	7/6.9/7	71.6	82.4	75.8
RQD (%)	87.10	20/17.4/-			
Average spacing of discontinuities (m)	0.72	15/21.9/-			
Density of discontinuities (m^{-1})	7.74	-/-/32.8			
Condition of discontinuities	Smooth surfaces, Separation 0.1-1 mm, slightly weathered walls	19.6/19.6/13.8			
Slake durability index (%)	98.74 - 99.44	-/-/10			
Groundwater condition	Completely dry	15/15/15			
Site 2					
Point load test ($I_{s(50)}$) (Mpa)	3.27 - 6.14 MPa	7/10.3/7	65	72.76	68.6
RQD (%)	44.20	12/8.8/-			
Average spacing of discontinuities (m)	0.48	11.6/19.2/-			
Density of discontinuities (m^{-1})	21.46	-/-/28.4			

Table 10. (cont.)

Parameters	Description or values	Rating: RMR_{89}/ M-RMR/RMR_{14}	RMR_{89}	M-RMR	RMR_{14}
Condition of discontinuities	Smooth surfaces, Separation <0.1 mm, slightly weathered walls	19.4/19.4/13			
Slake durability index (%)	97.99- 99.85	-/-/10			
Groundwater condition	Completely dry	15/15/15			
Site 3					
Point load test ($I_{s(50)}$) (Mpa)	2.82 – 7.41	7/9.1/7	72.7	82.9	75.3
RQD (%)	91.01	20/18.2/-			
Average spacing of discontinuities (m)	0.49	11.3/19.4/-			
Density of discontinuities (m^{-1})	7.28	-/-/30.3			
Condition of discontinuities	Smooth surfaces, Separation <0.1 mm, slightly weathered walls	20.5/20.5/13.5			
Slake durability index (%)	97.62 - 99.61	-/-/10			
Groundwater condition	Completely dry	15/15/15			

From the evaluation, all of the slopes fall under Class II of the RMR for RMR_{89} and RMR_{14}, and most of the slopes fall under Class I and Class II for M-RMR. Under the classification of RMR this would indicate the slopes to be of 'very good rock' for Class I and 'good rock' for Class II which under the classification would indicate generally good slope condition with long average stand-up time.

3.7 Geo-Resistivity and Geo-Engineering Properties of Granite

From the analysis, it was shown that deterioration of weathered granite results in measurable changes in electrical resistivity and engineering properties. From these, a comparison between the mapped electrical resistivity values with other published data of electrical resistivity range for weathered granite [16,20,44-46] is carried out: generally, the values fall under the acceptable range of observed electrical resistivity of weathered granite. As noted in earlier section, previous studies where the electrical resistivity values of weathered rock materials were directly correlated with prepared samples in the lab, such as the works by [41-43] are less common in the study of geotechnical properties of rock material, due to the use of measuring devices that are not commonly found in conventional engineering laboratory. Despite that, the range of electrical resistivity for the weathered granite could still be useful for classifying the different weathering grade of the granite found in the field, which have been shown to all have distinct engineering properties for the different grade of weathering. Similarly, a comparison between the results of engineering tests with published data of various engineering properties of weathered granite is carried out, where data is compared with values from the works of [47-53]. By comparing the results with the published studies, the values of engineering properties in this study falls roughly into the range of the commonly observed engineering properties of weathered granite. From this, an overall engineering properties index of weathered granite from the Karak-Lanchang is presented in Table 11.

Table 11. Summary of engineering properties index of weathered granite of Karak-Lanchang area

Weathering grade of granite, WG	Rock mass resistivity range (Ωm)	Specific gravity (g/cm^3)	Porosity & water content (%)	Ultrasonic pulse velocity (m/s)	Strength values
II	1000-3000	2.47-2.63	n: 0.80-5.90; MC: 0.31-2.39	4030.30-5316.58	Id_2: 97.62-99.85 % R: 42.0-64.0 PLS: 2.95-11.36 MPa UCS: 68.31-100.85 Mpa
III	400-1000	2.30-2.56	n: 1.65-12.10; MC: 1.33-5.17	3505.25-4794.37	Id_2: 91.29-99.98 % R: 34.6-44.8 PLS: 0.20-3.55 MPa UCS: 59.19-88.84 Mpa
IV	200-400	2.08-2.37	n: 8.06-20.75; MC: 4.49-9.55	511.35-1713.96	Id_2: 63.74-89.10 % R: 14-19.4 PLS: 0.06-0.36 MPa UCS: 5.56-17.99 Mpa
V	<200	1.77-2.29	n: 14.79-32.31; MC: 6.49-18.28	-	Id_2: 13.34 % PLS: 0.06 MPa R, UCS not available

n = porosity, MC = moisture content, Id_2 = Slake durability index, R = Schmidt Rebound Hammer value, PLS = point load strength, UCS = uniaxial compressive strength

4. CONCLUSION

Weathering process have resulted in various weathering grades of the granites of the slopes. The mapping of various discontinuity sets indicates the potential of kinematic failures. Petrographic analysis of the mineral content across the different weathering grade of the granite shows significant alteration of the mineral, noticeably the feldspars and biotite. Physical properties of the weathered granite show a decrease of the specific gravity of the granites with increasing weathering grade, whereas the porosity and moisture content of the granites show an increase with the increasing weathering grade. From statistical analysis, there are statistically significant strong increase in the value of porosity and moisture content with increase of weathering grade of granite, and statistically significant decrease of density, slake durability index, pulse velocity, surface hardness, point load strength and uniaxial strength with an increase of weathering grade of granite. Electrical resistivity mapping has identified up to five zones of weathering grade in the granite of the slopes, which correspond to observed features in the field. The mineral content, physical properties, and engineering properties of the weathered granite show comparable change with other literatures on weathered granite, where an increase of weathering grade in the rock gradually leads to the weakening of the physical properties and strength of the granite. This could then be attributed with a decrease in the measured electrical resistivity value. Result of the electrical resistivity mapping of the weathered granite indicate that the method is a useful addition for geotechnical assessment of rock slopes, where zones of weathering – and in turn, zones with weak strength properties – could be determined. This is useful in addition to conventional field engineering test of rock materials, which can be quite time consuming, high cost, and limited in covering the extent of the studied ground surface. Previous studies indicate how physical properties and engineering properties of rock material can be correlated with electrical resistivity value. By assessing the engineering properties of the granite of the cut slope from Lanchang-Karak area the rock mass classification of the rock slopes indicates them to be of very good to good quality (RMR Class I-Class II). However, with indication of potential wedge and toppling failure, and the presence of several zones of high weathering grade, the physical and engineering properties of the weathered material of the slopes should be observed for further deterioration and potential failures, especially along zones of high weathering indicated from field mapping and electrical resistivity mapping. An overall electrical resistivity and engineering properties index of the weathered granite is presented, which can be prove beneficial for future studies on the geotechnical assessment of weathered granite.

ACKNOWLEDGEMENT

The authors would like to thank the Faculty of Civil Engineering Technology for providing the experimental facilities and to all technicians at Soil Mechanics and Geotechnics Laboratory and Concrete and Material Laboratory.

FUNDING

The support provided by Universiti Malaysia Pahang in the form of a Geran Universiti Malaysia Pahang, grant number RDU190345, and the Postgraduate Research Grant Scheme, grant number PGRS2003207 for this study is highly appreciated.

AUTHOR CONTRIBUTIONS

Ahmad Faiz Salmanfarsi: Original draft preparation, Conceptualization, Methodology

Haryati Awang: Supervision

DATA AVAILABILITY STATEMENT

The data used to support the findings of this study are included within the article.

CONFLICTS OF INTEREST

The authors declare no conflict of interest.

References

[1] E. T. Mohamad, N. Latifi, A. Arefnia, and M. F. Isa, "Effects of moisture content on the strength of tropically weathered granite from Malaysia," *Bulletin of Engineering Geology and the Environment*, vol. 75, pp. 369–390, 2016.

[2] J. S. Lee, and H. K. Yoon, "Characterization of rock weathering using elastic waves: a laboratory-scale experimental study," *Journal of Applied Geophysics*, vol. 140, pp. 24–33, 2017.

[3] A. L. Little, "The engineering classification of residual tropical soils," *Proceeding of 7th International Conference Soil Mechanics & Foundation Engineering*, (Mexico), vol. 1, pp. 1–10, 1969.

[4] W. R. Dearman, "Weathering classification in the characterisation of rock: A revision," *Bulletin of Engineering Geology & the Environment*, vol. 14, pp. 123–127, 1975.

[5] J. K. Raj, “Physical characterization of a deep weathering profile over rhyolite in humid tropical Peninsular Malaysia,” *Geotechnical and Geological Engineering*, vol. 36, no. 6, pp. 3793-3809, 2018.

[6] H. Awang, A. F. Salmanfarsi, A. Ariizam, and Ali, M. I. “Engineering characterisation of weathered rock at Sri Jaya, Pahang, Malaysia,” *IOP Conference Series: Earth and Environmental Science*, vol. 682, pp. 012016, 2021.

[7] P. B. Durgin, “Landslides and the weathering of granitic rocks,” *Geological Society of America Reviews in Engineering Geology*, vol. 3, pp. 127-31, 1977.

[8] H. Abdul Rahman, and J. Mapjabil. “Landslides disaster in Malaysia: An overview,” *Health Environmental Journal*, vol, 8, pp. 58-71, 2017.

[9] M. Al-Bared, R. Abdullah, N. Z. Mohd Yunus, M. Mohd Amin, and H. Awang, “Rock slope assessment using kinematic and numerical analyses,” *Jurnal Teknologi (Sciences & Engineering)*, vol. 77, pp. 59-66, 2015.

[10] S. K. Nagendran, M. A. Mohamad Ismail, and Y. T. Wen, “2D And 3D rock slope stability assessment using limit equilibrium method incorporating photogrammetry technique,” *Bulletin of the Geological Society of Malaysia*, vol. 68, pp. 133-139, 2019.

[11] M. H. Zakaria, K. M. Idris, Z. Majid, M. F. M. Ariff, N. Darwin, M. A. Abbas, et al., “Practical terrestrial laser scanning field procedure and point cloud processing for bim applications - Tnb control and relay room 132/22KV,” *ISPRS*, vol. 42, no. 4/W16, pp. 705-710, 2019.

[12] H. Basahel, and H.Mitri, “Application of rock mass classification systems to rock slope stability assessment: A case study,” *Journal of Rock Mechanics and Geotechnical Engineering*, vol. 9, pp. 993–1009, 2017.

[13] A. F. Abdul Rahim, A. G. Md Rafek, A. S. Serasa, A. R. Jaapar, T. L. Goh, R. Roslee, et al., “A review of rock slope stability assessment practice in Malaysia,” *Sains Malaysiana*, vol. 52, no. 2, pp. 399-416, 2023.

[14] S. Anbazhagan, V. Ramesh, and S. E. Saranaathan, “Cut slope stability assessment along ghat road section of Kolli hills, India,” *Natural Hazards*, vol. 86, no. 3, pp. 1081–1104, 2017.

[15] S. D. Priest, “*Discontinuity analysis for rock engineering*,” Chapman & Hall, 1993.

[16] H. Awang, R. A. Abdullah, and S. A. Samad, “Ground investigation using 2D resistivity imaging for road construction,” *Jurnal Teknologi (Sciences & Engineering)*, vol. 78, pp. 81–5, 2016.

[17] M. H. Arifin, T. A. Jamaluddin, H. Husin, A. Ismail, A. A. Abbas, M. N. Mohd Nordin, et al., “Comparison of geological mapping with electrical resistivity and ground penetration radar methods for rock fractured system study,” *Chiang Mai Journal of Science*, vol. 43, pp. 1346–1357, 2016.

[18] M. Junaid, R. A. Abdullah. R. Saa’ri, M. Alel, W. Ali, and A. Ullah, “Recognition of boulder in granite deposit using integrated borehole and 2D electrical resistivity imaging for effective mine planning and development,” *Bulletin of the Geological Society of Malaysia*. vol. 67, pp. 99–104, 2019.

[19] H. Hussin, M. H. Arifin, T. A. Jamaluddin, M. F. Abdul Ghani, N. Ismail, and A. M. Abdullah, “Integration of field mapping, lineament interpretation and electrical resistivity tomography survey to characterize granitic rock mass lining by shotcrete,” *Bulletin of the Geological Society of Malaysia*, vol. 69, pp. 39–51, 2020.

[20] O. P. Olabode, L. H. San, and M. H. Ramli, “Analysis of geotechnical-assisted 2-D electrical resistivity tomography monitoring of slope instability in residual soil of weathered granitic basement,” *Frontiers in Earth Science*, vol. 7, p. 580230, 2020.

[21] H. Awang, A. F. Salmanfarsi, M. S. I. Zaini, M. A. F. Mohamad Yazid, and Ali, M. I. “Investigation of groundwater table under rock slope by using electrical resistivity imaging at Sri Jaya, Pahang, Malaysia,” *IOP Conference Series: Earth and Environmental Science*, vol. 682, p. 012017, 2021.

[22] C. S. Hutchison, and D. N. K. Tan, *Geology of Peninsular Malaysia*, Kuala Lumpur: University of Malaya & Geological Society of Malaysia, 2009.

[23] N. Simon, J. Mat Akhir, A. Napiah, and H. K. Tan, “Development of landslide database along km 160 – km 190, East Coast Highway, Pahang,” *Warta Geologi*, vol. 34, no. 5&6, pp. 233–238, 2008.

[24] H. K. Tan, J. Mat Akhir, A. Napiah, and N. Simon, “Pemetaan ramalan potensi tanah runtuh di sepanjang km160-190 Lebuhraya Pantai Timur dengan pendekatan Sistem Maklumat Geografi: Kaedah statistik,” *Warta Geologi*, vol. 34, no. 5&6, pp. 239–242, 2008.

[25] M. Gasparon, and R. Varne, “Sumatran granitoids and their relationship to Southeast Asian terranes,” *Tectonophysics*, vol. 251, pp. 277–299, 1995.

[26] E. J. Cobbing, P. E. J. Pitfield, D. P. F. Darbyshire, and D. I. J. Mallick, “The granites of the South-East Asian tin belt,” London: HMSO, 1992.

[27] M. O. Schwartz, S. S. Rajah, A. K. Askury, P. Putthapiban, and S. Djaswadi, “The Southeast Asian tin belt,” *Earth-Science Reviews*, vol. 38, pp. 95-293, 1995.

[28] R. D. Nugraheni, D. Sunjaya, and S. Agustini, “Regional tectonic and geochemical approach to distinguish bauxite characteristics in Pahang, Malaysia and West Kalimantan, Indonesia,” *IOP Conference Series: Earth and Environmental Science*, vol. 212, p. 012026, 2018.

[29] A. A. Ghani, M. Shahjamal, T. F. Ng, N. E. H. Ismail, M. T. Mohamad Zulkifley, N. N. Islami, et al., “Ce Anomaly in I–Type Granitic Soil from Kuantan, Peninsular Malaysia: Retention of zircon in the weathering product,” *Sains Malaysiana*, vol. 48, no. 2, pp. 309–315, 2019.

[30] British Standards Institution, “*Geotechnical investigation and testing. Identification, description and classification of rock. Part 1: Identification and description. BS EN ISO 14689:2018*,” London: BSI, 2018.

[31] British Standards Institution, “*Code of Practice for Site Investigations. BS 5930: 2015+A1:2020*,” London: BSI, 2015.

[32] R. Ulusay, and J. A. Hudson, *The complete ISRM suggested methods for rock characterization, testing and monitoring: 1974-2006*, Ankara: International Society of Rock Mechanics Commission on Testing Methods, 2007.

[33] U. Hamzah, R. Yaacup, A. R. Samsudin, and M. S. Ayub, “Electrical imaging of the groundwater aquifer at Banting, Selangor, Malaysia,” *Environmental Geology*, vol. 49, pp. 1156-1162, 2006.

[34] R. Ulusay, *The ISRM Suggested Methods for Rock Characterization, Testing and Monitoring: 2007-2014*, Switzerland: Springer International Publishing, 2015.

[35] E. Hoek, and J. W. Bray, *Rock Slope Engineering*, Institute of Mining and Metallurgy, 1981. doi:10.1201/9781482267099

[36] Y. Admassu, *User’s Guide DipAnalyst 2.0 for Windows-software for kinematic analysis of rock slopes*, 2012.

[37] Rocscience Inc., *Dip v. 6.0 - graphical and statistical analysis of orientation data*, Toronto, 2014.

[38] Z. T.Bieniawski, *Engineering rock mass classifications: A complete manual for engineers and geologists in mining, civil, and petroleum engineering*, John Wiley & Sons, New York, 1989.

[39] Z. Şen, amd B. H. Sadagah, “Modified rock mass classification system by continuous rating,” *Engineering Geology*, vol. 67, no. 3-4, pp. 269-280, 2003.

[40] B. Celada, I. Tardáguila, P. Varona, A. Rodríguez, and Z. T. Bieniawski, “Innovating tunnel design by an improved experience-based RMR system,” In A. Negro, M. O. Cecilio Jr. & W. Bilfinger (Eds.), P*roceedings of the World Tunnel Congress*, pp. 1–9, 2014.

[41] S. Kahraman, and T. Yeken, “Electrical resistivity measurement to predict uniaxial compressive and tensile strength of igneous rocks,” *Bulletin of Materials Science*, vol. 33, pp. 731–735, 2010.

[42] O. Su, and M. Momayez “Indirect estimation of electrical resistivity by abrasion and physico-mechanical properties of rocks,” *Journal of Applied Geophysics*, vol. 143, pp. 23–30, 2017.

[43] I. Sertcelik, C. Kurtulus, F. Sertçelik, E. Peksen, and M. Asci, “Investigation of relations between physical and electrical properties of rocks and concretes,” *Journal of Applied Geophysics*, 15 142–52, 2018.

[44] J. Olona, J. A. Pulgar, G. Fernández-Viejo, C. López-Fernández, and J. M. González-Cortina, “Weathering variations in a granitic massif and related geotechnical properties through seismic and electrical resistivity methods,” *Near Surface Geophysics*, vol. 8, pp. 585–599, 2010.

[45] S. Almadani, E. Ibrahim, A. Al-Amri, M. Fnais, and K. Abdelrahman, “Delineation of a fractured granite aquifer in the Alwadeen area, Southwest Saudi Arabia using a geoelectrical resistivity survey,” *Arabian Journal of Geosciences*, vol. 12, pp. 449, 2019.

[46] M. S. I. Zaini, M. F. Ishak, M. F. Zolkepli, M. S. Wahap, J. I. Jaafar Sidek, A. Mohd Yasin, et al., “Granite exploration by using Electrical Resistivity Imaging (ERI): A case study in Johor,” *International Journal of Integrated Engineering*, vol. 12, pp. 328–347, 2020.

[47] E. T. Mohamad, N. Gofar, M. F. Mohd. Amin, and M. F. Mohd. Isa, “Field assessment of rock strength by impact load test,” *Malaysian Journal of Civil Engineering*, vol. 23, pp. 105–110, 2011.

[48] T. L. Goh, A. G. Rafek, and M. H. Arifin, “Geomechanical strength of granites and schists of Peninsular Malaysia,” *Sains Malaysiana*, vol. 41, no. 2., pp. 193–198, 2012.

[49] A. Momeni, G. R. Khanlari, M. Heidari, A. A. Sepahi, and E. Bazvand, “New engineering geological weathering classifications for granitoid rocks,” *Engineering Geology*, vol. 185, pp. 43–51, 2015.

[50] M. Sajid, J. Coggan, M. Arif, J. Andersen, and G. Rollinson, “Petrographic features as an effective indicator for the variation in strength of granites,” *Engineering Geology*, vol. 202, pp. 43–54, 2016.

[51] A. F. Jobli, A. Z. Hampden, and R. Tawie, “The role of ultrasonic velocity and Schmidt hammer hardness - The simple and economical non-destructive test for the evaluation of mechanical properties of weathered granite,” *AIP Conference Proceedings*, vol. 1875, p. 030005, 2017.

[52] A. Momeni, S. S. Hashemi, G. R. Khanlari, and M. Heidari, “The effect of weathering on durability and deformability properties of granitoid rocks,” *Bulletin of Engineering Geology and the Environment*, vol. 76, pp. 1–13, 2017.

[53] Z. Wengang, H. Liang, Z. Zixu, and Z. Yanmei, “Digitalization of mechanical and physical properties of Singapore Bukit Timah Granite Rocks based on borehole data from four sites,” *Underground Space*, vol. 6, no. 5, pp. 483–491, 2021.